Recursive Least-Squares Filtering of Pseudorange Measurements

A.Q. Le and P.J.G. Teunissen
Delft Institute of Earth Observation and Space Systems (DEOS)
Delft University of Technology - the Netherlands

Abstract

Code pseudorange measurement noise is one of the major error sources in Precise Point Positioning. A recursive least-squares solution with proper functional and stochastic modelling would help to exploit in addition the ultra high precision of the carrier phase measurement. Analyses of different methods, including phase smoothed, phase connected and phase adjusted pseudorange algorithm, will show that the phase adjusted pseudorange algorithm is statistically optimal. Static and kinematic experiment results also support the conclusion with more than 30% of improvement by going from the phase smoothed to the phase adjusted algorithm.

1 Introduction

In standalone positioning such as standard GPS positioning, Wide Area Differential GPS (WADGPS) positioning or Precise Point Positioning (PPP), the prime observation type is the code pseudorange. The main sources of error in this positioning mode include satellite orbits and clocks, the ionosphere, the troposphere, and the pseudorange errors (noise and multipath). While the first three error sources can be mitigated by augmentation corrections or products from a network of reference stations (as done in WADGPS and PPP), the pseudorange errors *cannot* since they are *local* effects. In this case, the extremely precise carrier phase measurement can come to rescue.

The noise can be reduced with carrier phase by using the popular Hatch smoothing algorithm. However, this is not an optimal solution as it is based on a channel-by-channel basis. Instead, a recursive least-squares filter which can be proven to be statistically optimal will be deployed, namely the phase-adjusted pseudorange algorithm.

The algorithm takes both pseudorange and carrier phase measurements in one integral least-squares solution where carrier phase ambiguities are considered as constant but unknown parameters. The positioning parameters together with carrier phase ambiguities are estimated recursively. This processing scheme minimises computational load and all information is preserved. The algorithm can be applied to any kind of GPS positioning where both pseudorange and carrier phase are involved.

In this paper, Precise Point Positioning will be implemented with the phase-adjusted pseudorange algorithm and a comparison to other smoothing approaches will be made. Although the results are post-processed due to the current availability of global data products,

the processing engine is purely kinematic (no dynamic assumption needed) and suitable for real-time applications. In fact real-time operation has been emulated in this paper.

Results to be presented in the paper are of long-term static data from several stations around the world with different GPS receivers, as well as from kinematic experiments. In general, the obtained accuracy is at sub-metre level worldwide. Under favourable conditions, it can reach 40 centimetres horizontally and 60 centimetres vertically (at the 95% level). The results also show a large improvement going from the classical Hatch smoothing algorithm to the phase-adjusted pseudorange algorithm. It will be shown that the 95% positioning error can be improved by about 30-50%.

2 Filtering methods using carrier phase measurements

2.1 Classical phase smoothing algorithm

The classical phase smoothing algorithm [1] was introduced by Hatch (1982) and is still widely used nowadays due to the simplicity and flexibility of the algorithm. The recursive formula of the algorithm reads:

$$\widehat{P}_k = \frac{1}{k} P_k + \frac{k-1}{k} \left(\widehat{P}_{k-1} + \delta\Phi_{k,k-1} \right) \tag{1}$$

with $\widehat{P}_k$ the phase-smoothed pseudorange at epoch t_k; P_k the pseudorange observation at epoch t_k; $\widehat{P}_{k-1}$ the phase-smoothed pseudorange at epoch t_{k-1}; $\delta\Phi_{k,k-1} = \Phi_k - \Phi_{k-1}$ the time-differenced carrier phase observation; Φ_k the carrier phase observation at epoch t_k; Φ_{k-1} the carrier phase observation at epoch t_{k-1}. Note that all the carrier phase observations are in units of range.

The same smoothed pseudorange equation can be expressed in a different form as a linear combination of the previous epochs'observations, including both pseudorange and carrier phase:

$$\widehat{P}_k = \frac{1}{k} \sum_{i=1}^{k} P_i - \frac{1}{k} \sum_{i=1}^{k} \Phi_i + \Phi_k \tag{2}$$

If the denote x_i and A_i are the vector of unknown parameters and its design matrix at epoch i, and ∇ is the vector of ambiguities (unchanged over time), the observation equations at epoch i can be written:

$$E\{ \begin{pmatrix} \underline{P}_i \\ \underline{\Phi}_i \end{pmatrix} \} = \begin{pmatrix} A_i & 0 \\ A_i & I \end{pmatrix} \begin{pmatrix} x_i \\ \nabla \end{pmatrix} \tag{3}$$

From (2) and (3), we have:

$$\begin{aligned} E\{\underline{\widehat{P}}_k\} &= \frac{1}{k} \sum_{i=1}^{k} A_i x_i - \frac{1}{k} \sum_{i=1}^{k} (A_i x_i + \nabla) + A_k x_k + \nabla \\ &= A_k x_k \end{aligned} \tag{4}$$

[1] Strictly, *smoothing* implies the computation of estimates for unknowns parameters (e.g. position coordinates) pertaining to epoch t_k, using observations from the whole data collection period, i.e. $[t_1, t_l]$ with $1 \leq k \leq l$; the data period extends beyond epoch t_k. *Filtering* refers to estimates for parameters at epoch t_k, using solely data up to and including epoch t_k, i.e. $[t_1, t_k]$. Filtering allows real-time operation and smoothing does not. In this paper, we continue to refer to 'phase smoothing', as commonly done, but strictly filtering is meant instead.

with $E\{.\}$ the mathematical expectation operator.

As shown in (4), through the linear combination, the design matrix for the smoothed pseudorange is preserved when no cycle slips occur. However, the variance matrix is no longer (block) diagonal and hence, recursive computation is not possible for this model.

It can be seen clearly when taking the first k epochs into account. The smoothed pseudoranges on the left form the system:

$$\begin{pmatrix} \widehat{\underline{P}}_1 \\ \widehat{\underline{P}}_2 \\ \vdots \\ \widehat{\underline{P}}_{k-1} \\ \widehat{\underline{P}}_k \end{pmatrix} = \begin{pmatrix} I & 0 & 0 & 0 & \dots & & \dots & 0 & 0 \\ \frac{I}{2} & -\frac{I}{2} & \frac{I}{2} & \frac{I}{2} & 0 & & \dots & 0 & 0 \\ \vdots & & & & \ddots & & & \vdots & \vdots \\ \frac{I}{k-1} & -\frac{I}{k-1} & \dots & & \dots & \frac{I}{k-1} & \frac{(k-2)I}{k-1} & 0 & 0 \\ \frac{I}{k} & -\frac{I}{k} & \dots & & \dots & \frac{I}{k} & -\frac{I}{k} & \frac{I}{k} & \frac{(k-1)I}{k} \end{pmatrix} \begin{pmatrix} \underline{P}_1 \\ \underline{\Phi}_1 \\ \underline{P}_2 \\ \underline{\Phi}_2 \\ \vdots \\ \underline{P}_{k-1} \\ \underline{\Phi}_{k-1} \\ \underline{P}_k \\ \underline{\Phi}_k \end{pmatrix} \tag{5}$$

Assuming no (cross and time) correlation between the original code and phase observations and that code and phase variances are Q_P and Q_Φ at every epoch, application of the propagation law gives the variance of the smoothed pseudoranges:

$$D\{\} = \begin{pmatrix} Q_P & \frac{Q_P}{2} & \dots & \frac{Q_P}{(k-1)} & \frac{Q_P}{k} \\ \frac{Q_P}{2} & \frac{Q_P}{2} & & \vdots & \vdots \\ \vdots & \vdots & \ddots & \vdots & \vdots \\ \frac{Q_P}{(k-1)} & \frac{Q_P}{(k-1)} & \dots & \frac{Q_P}{(k-1)} & \frac{Q_P}{k} \\ \frac{Q_P}{k} & \frac{Q_P}{k} & \dots & \frac{Q_P}{k} & \frac{Q_P}{k} \end{pmatrix} + \begin{pmatrix} 0 & & & & 0 \\ & \frac{Q_\Phi}{2} & & & \\ & & \ddots & & \\ & & & \frac{(k-2)Q_\Phi}{(k-1)} & \\ 0 & & & & \frac{(k-1)Q_\Phi}{k} \end{pmatrix} \tag{6}$$

Based on the smoothed pseudoranges, subsequent recursive processing is usually carried out to obtain estimates for the receiver position, epoch-after-epoch. However, there is clearly (extremely) high time-correlation between the smoothed pseudoranges, which prevents the model to work recursively. The correlation is obviously ignored in the smoothing algorithm.

2.2 Phase-connected pseudorange algorithm

Another newly developed algorithm using the carrier phase to smooth the pseudorange was from Bisnath et al (2002), in which differenced carrier phase measurements between epochs are used as additional observation next to the pseudorange. As long as no cycle slips occur, ambiguity parameters are absent. For a single epoch, the observation equations are given:

$$\begin{aligned} E\{\begin{pmatrix} \underline{P}_k \\ \delta\underline{\Phi}_{k,k-1} \end{pmatrix}\} &= \begin{pmatrix} 0 & A_k \\ -A_{k-1} & A_k \end{pmatrix} \begin{pmatrix} x_{k-1} \\ x_k \end{pmatrix} \\ D\{\begin{pmatrix} \underline{P}_k \\ \delta\underline{\Phi}_{k,k-1} \end{pmatrix}\} &= \begin{pmatrix} Q_{P_k} & 0 \\ 0 & Q_{\Phi_{k,k-1}} \end{pmatrix} \end{aligned} \tag{7}$$

where $\underline{P}_k$ the linearised pseudorange observation; $\delta\underline{\Phi}_{i,i-1} = \underline{\Phi}_i - \underline{\Phi}_{i-1}$ the linearised time-differenced carrier phase observation. By linearised we mean 'observed minus computed' following from the linearisation of the original non-linear functional relation.

Again, taking k epochs together, the full model of observation equations is:

$$E\{\begin{pmatrix} \underline{P}_1 \\ \delta\underline{\Phi}_{21} \\ \underline{P}_2 \\ \delta\underline{\Phi}_{32} \\ \vdots \\ \delta\underline{\Phi}_{k,k-1} \\ \underline{P}_k \end{pmatrix}\} = \begin{pmatrix} A_1 & & & & & \\ -A_1 & A_2 & & & & \\ & A_2 & & & & \\ & -A_2 & A_3 & & & \\ & & & \ddots & & \\ & & & & -A_{k-1} & A_k \\ & & & & & A_k \end{pmatrix} \begin{pmatrix} x_1 \\ x_2 \\ \vdots \\ x_k \end{pmatrix} \tag{8}$$

Vector x_k primarily contains the receiver position coordinates but other parameters could be included as well, as for instance the receiver clock error. With the same assumption of no correlation between (undifferenced) pseudorange and carrier phase measurements as above, the variance matrix can be derived for the observation vector in (8):

$$D\{\} = \begin{pmatrix} Q_{P_1} & & & & & & & 0 \\ & Q_{\Phi_{21}} & 0 & -Q_{\Phi_2} & & & & \\ & & Q_{P_2} & & & & & \\ & -Q_{\Phi_2} & 0 & Q_{\Phi_{32}} & 0 & -Q_{\Phi_3} & & \\ & & & & \ddots & & & \\ & & & & & \ddots & & \\ & & & & -Q_{\Phi_{k-1}} & 0 & Q_{\Phi_{k,k-1}} & \\ 0 & & & & & & & Q_{P_k} \end{pmatrix} \tag{9}$$

with $Q_{\Phi_{i,i-1}} = Q_{\Phi_i} + Q_{\Phi_{i-1}}$.

Similar to that of the Hatch smoothing algorithm, this matrix is not (block) diagonal though the correlation is not as heavy as that of the first algorithm. Strictly speaking, the system (8) and (9) cannot be recursively solved to obtain estimates for the position coordinates. One assumption has been made that all the resulting time correlation (due to the differenced carrier phase observations) is neglected. In this case, the system can be solved recursively (see Le (2004)).

2.3 Phase-adjusted pseudorange algorithm

The optimal solution would be a model where all the observations (including carrier phase measurements) are put into a unique model of observation equations. This is the model where all the information should be preserved and the unknowns at each epoch can be computed by a recursive least-squares solution. Based on this criterion, the phase-adjusted pseudorange algorithm was developed by Teunissen (1991). In this model, all original (undifferenced) pseudorange and carrier phase measurements are the basic observations; the unknowns including ambiguities and positioning parameters are recursively estimated.

$$E\{\begin{pmatrix} \underline{P}_1 \\ \underline{\Phi}_1 \\ \underline{P}_2 \\ \underline{\Phi}_2 \\ \vdots \\ \underline{P}_k \\ \underline{\Phi}_k \end{pmatrix}\} = \begin{pmatrix} A_1 & & & & 0 \\ A_1 & & & & I \\ & A_2 & & & 0 \\ & A_2 & & & I \\ & & \ddots & \vdots & \\ & & & A_k & 0 \\ & & & A_k & I \end{pmatrix} \begin{pmatrix} x_1 \\ x_2 \\ \vdots \\ x_k \\ \nabla \end{pmatrix} \tag{10}$$

with $\underline{P}_i$ the vector of linearised pseudoranges at epoch t_i; $\underline{\Phi}_i$ the vector of linearised carrier phases at epoch t_i; x_i the vector of unknown parameters at epoch t_i; A_i the linearised design matrix at epoch t_i; and ∇ the vector of unknown ambiguities (assumed to be time-invariant for simplicity in this explanation).

$$D\{\begin{pmatrix} \underline{P}_1 \\ \underline{\Phi}_1 \\ \underline{P}_2 \\ \underline{\Phi}_2 \\ \vdots \\ \underline{\Phi}_{k-1} \\ \underline{P}_k \\ \underline{\Phi}_k \end{pmatrix}\} = \begin{pmatrix} Q_{P_1} & & & & & & & 0 \\ & Q_{\Phi_1} & & & & & & \\ & & Q_{P_2} & & & & & \\ & & & Q_{\Phi_2} & & & & \\ & & & & \ddots & & & \\ & & & & & Q_{\Phi_{k-1}} & & \\ & & & & & & Q_{P_k} & \\ 0 & & & & & & & Q_{\Phi_k} \end{pmatrix} \tag{11}$$

with Q_{P_i} variance matrix of code measurements at epoch t_i and Q_{Φ_i} variance matrix of carrier phase measurements.

The recursive equations for the position parameters (and possibly others as well) can be given as (12):

$$\begin{aligned} \underline{\hat{x}}_k &= Q_{\hat{x}_k} A_k^T (Q_{P_k}^{-1} \underline{P}_k + [Q_{\Phi_k} + Q_{\hat{\nabla}_{k-1}}]^{-1} [\underline{\Phi}_k - \hat{\nabla}_{k-1}]) \\ Q_{\hat{x}_k} &= [A_k^T (Q_{P_k}^{-1} + [Q_{\Phi_k} + Q_{\hat{\nabla}_{k-1}}]^{-1}) A_k]^{-1} \end{aligned} \tag{12}$$

The update for the ambiguities is also needed to fulfill the recursive solution:

$$\begin{aligned} \underline{\hat{\nabla}}_k &= \underline{\hat{\nabla}}_{k-1} + Q_{\underline{\hat{\nabla}}_{k-1}} [Q_{P_k} + Q_{\underline{\hat{\nabla}}_{k-1}}]^{-1} [\underline{\Phi}_k - \underline{\hat{\nabla}}_{k-1} - A_k \underline{\hat{x}}_k] \\ Q_{\hat{\nabla}_k} &= Q_{\hat{\nabla}_{k-1}} - Q_{\hat{\nabla}_{k-1}} [Q_{\Phi_k} + Q_{\hat{\nabla}_{k-1}}]^{-1} Q_{\hat{\nabla}_{k-1}} \\ &\quad + Q_{\hat{\nabla}_{k-1}} [Q_{\Phi_k} + Q_{\hat{\nabla}_{k-1}}]^{-1} A_k Q_{\hat{x}_k} A_k^T [Q_{\Phi_k} + Q_{\hat{\nabla}_{k-1}}]^{-1} Q_{\hat{\nabla}_{k-1}} \end{aligned} \tag{13}$$

The initial epoch's parameters $\underline{\hat{x}}_1$ and $\underline{\hat{\nabla}}_1$ with $Q_{\hat{x}_1}$ and $Q_{\hat{\nabla}_1}$ follow from a least-squares solution based on P_1 and Φ_1.

This algorithm is optimal from a statistical point of view since it properly treats the model as a whole (with all observations of all epochs). No further assumption is made beside the

assumption of no time correlation between epochs. The algorithm is purely kinematic as no dynamic model is needed for the receiver. On the other hand, if such information is available, it can be easily incorporated.

3 Experimental results with Precise Point Positioning

In standalone positioning, the main error sources are satellite orbits and clocks, the ionosphere, the troposphere and the pseudorange noise. The first three sources can be compensated for in Precise Point Positioning (PPP) by using publicly available products, such as precise ephemerides, Global Ionosphere Maps (GIM) and a precise tropospheric model. Not as such, the code noise cannot be eliminated in a similar way and is significantly large in this mode of positioning. Hence, PPP benefits a lot from filtering using carrier phase measurements to mitigate the noise of pseudorange measurements as outlined in the previous section. Various experiments were carried out with the phase-adjusted pseudorange algorithm, both static and kinematic.

In all experiments of this paper, the *single-frequency* PPP approach using publicly available products was implemented. The corrections/models in use include precise orbits and clocks from International GPS Services (IGS), GIMs from Center for Orbit Determination in Europe (CODE) and the Saastamoinen tropospheric model. An elevation angle dependent weighting scheme is used for both code and phase measurements. Le (2004) describes the approach in more detail.

3.1 With static receivers

An extensive static test of one week was performed with 4 stations, namely DELF, EIJS, DUBO and HOB2. The first two stations are part of the AGRS.NL network in the Netherlands while the other two belong to the IGS network, one (DUBO) in Canada and one (HOB2) in Australia. Data were collected with 30-second interval. Table 1 shows the results for the phase-adjusted pseudorange algorithm. In general, the accuracy is about half a metre horizontally and one metre vertically. Better results are obtained in Europe and (possibly) in North America thanks to better quality of the GIMs.

	DELF	**EIJS**	**DUBO**	**HOB2**
North	0.45	0.41	0.78	0.53
East	0.44	0.42	0.59	0.72
Up	0.88	0.82	1.01	1.39

Table 1: Extensive static test results [m]. 95%-value (95^{th} percentile) of position errors in local North, East and Up coordinates (with respect to known coordinates of the markers) with one week of data at 30-second interval for 4 different locations around the world.

A comparison between the three algorithms was made from 24 hours data collected at the DELF station. Again, a 30-second interval was used. Table 2 shows about 30% improvement by going from the Phase smoothing to the Phase adjusted algorithm in the North and vertical direction. The accuracies of all algorithms in the East component are comparable.

The horizontal scatters and time-series of the three components, North, East and Up are plotted in figure 1 and 2. The 'no smooth' solution is also included for reference (using solely pseudorange observations).

Note that the phase smoothed algorithm was implemented with different window lengths. It can be seen that for large sampling intervals (e.g. 30 seconds), the phase smoothed algorithm is sensitive to the window length choice. As shown in table 2, it should be about 5 epochs (at 30-sec interval) or equivalent to 2-3 minutes.

	No smooth	**Phase smoothed**			**Phase connected**	**Phase adjusted**
		3	5	8		
North	0.71	0.59	0.59	0.67	0.49	0.43
East	0.49	0.37	0.36	0.39	0.32	0.42
Up	1.10	0.95	0.95	1.13	0.76	0.74

Table 2: Static test results at DELF [m]. 95%-value of position estimates in local North, East and Up coordinates with one day of data at 30-second interval for 4 different approaches (Phase smoothed algorithm with different window lengths - 3, 5, 8 epochs)

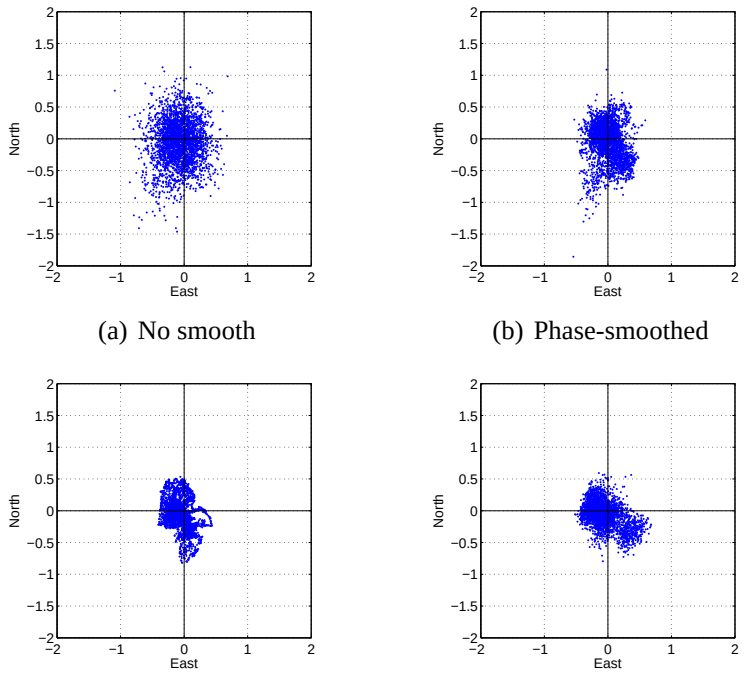

(a) No smooth (b) Phase-smoothed

(c) Phase-connected (d) Phase-adjusted

Figure 1: Horizontal scattered error. DELF station, 24-hour, 30-sec interval data with 4 different approaches (phase smoothed algorithm with 5-epoch window length).

3.2 With kinematic receivers

A maritime kinematic experiment was carried out with a small boat on Schie river (between Delft and Rotterdam, the Netherlands). Nearly 3 hours (1 Hz) of kinematic data from 2 re-

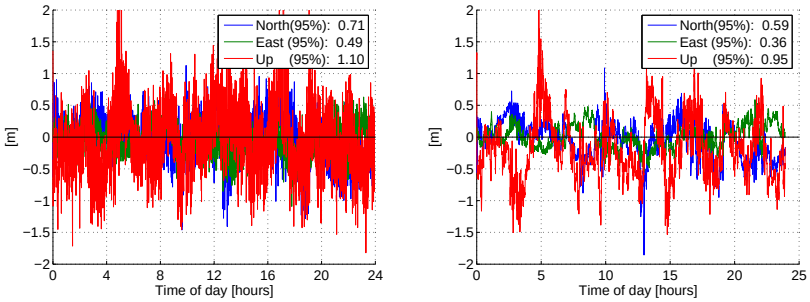

(a) No smooth

(b) Phase-smoothed

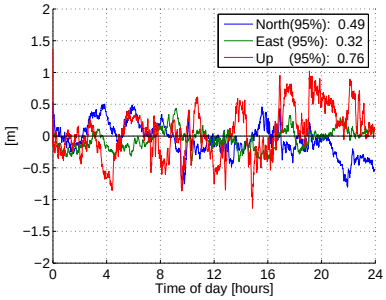

(c) Phase-connected

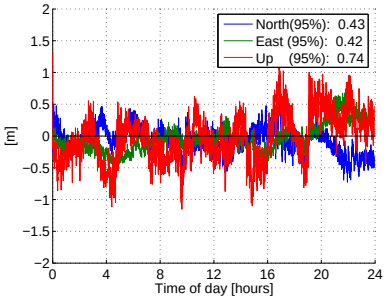

(d) Phase-adjusted

Figure 2: North, East and Up errors. DELF station, 24-hour, 30-sec interval data with 4 different approaches (phase smoothed algorithm with 5-epoch window length).

ceivers, namely Ashtech Z-XII3 and Leica SR530 were collected. The cm-accuracy reference trajectories were computed in a (dual-frequency carrier phase) differential GPS solution with a reference station nearby (only few kilometres away). Again, the three algorithms' results are included in table 3. The window length used in the phase smoothed algorithm is 100-second.

Receiver		**Phase smoothed**	**Phase connected**	**Phase adjusted**
Ashtech	North	1.12	0.54	0.45
	East	0.39	0.31	0.29
	Up	1.20	0.88	0.84
Leica	North	0.79	0.48	0.39
	East	0.36	0.28	0.34
	Up	0.83	0.76	0.56

Table 3: Kinematic results [m]. 95%-value of position estimates in local North, East and Up coordinates with 2 receivers for 3 different approaches, 3 hours of data at one-second interval (Phase smoothed algorithm with 100-epoch window length)

In the kinematic results, the accuracy is improved by more than 50% in the North component. Significant differences also can be seen in other components of about 30-50% (see figure 3 to 6), especially with the Ashtech receiver.

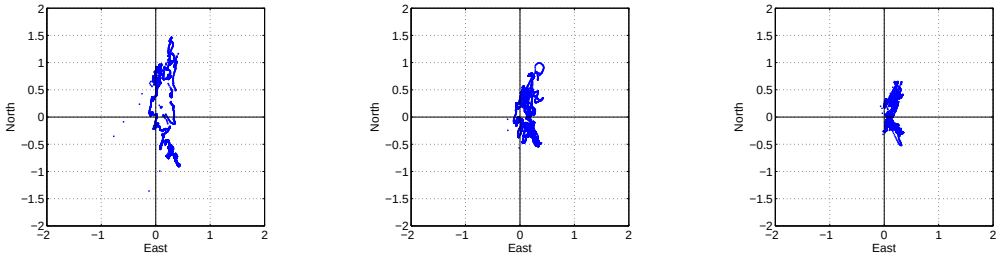

(a) Phase-smoothed (b) Phase-connected (c) Phase-adjusted

Figure 3: Horizontal scattered error. Ashtech ZXII3 kinematic receiver, 3-hour, 1-sec interval data with 3 different approaches (phase smoothed algorithm with 100-epoch window length).

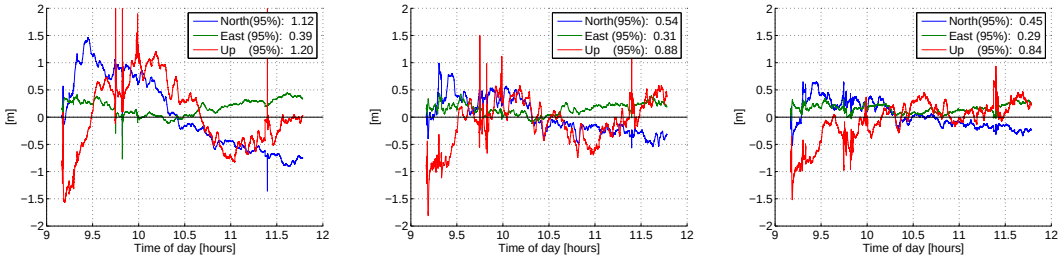

(a) Phase-smoothed (b) Phase-connected (c) Phase-adjusted

Figure 4: North, East and Up errors. Ashtech ZXII3 kinematic receiver, 3-hour, 1-sec interval data with 3 different approaches (phase smoothed algorithm with 100-epoch window length).

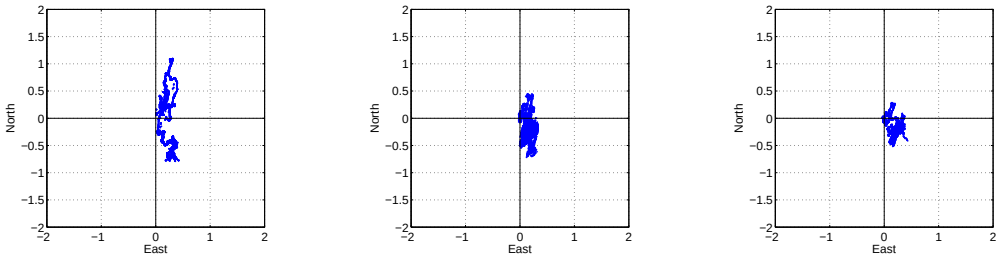

(a) Phase-smoothed (b) Phase-connected (c) Phase-adjusted

Figure 5: Horizontal scattered error. Leica SR530 kinematic receiver, 3-hour, 1-sec interval data with 4 different approaches (phase smoothed algorithm with 100-epoch window length).

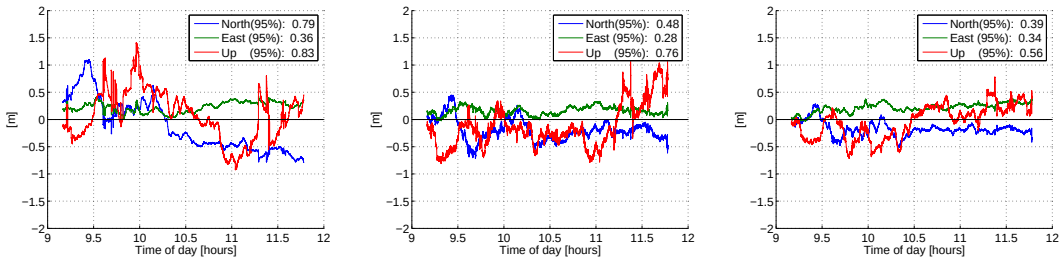

(a) Phase-smoothed (b) Phase-connected (c) Phase-adjusted

Figure 6: North, East and Up errors. Leica SR530 kinematic receiver, 3-hour, 1-sec interval data with 4 different approaches (phase smoothed algorithm with 100-epoch window length).

4 Conclusions

The Phase-adjusted pseudorange algorithm, statistically optimal, is a fully kinematic filter. It has been demonstrated to work robustly in various circumstances, from static to kinematic, over short time spans and long time spans. The accuracy of its application in single-frequency PPP, in general, can be confirmed at half a metre horizontally and one metre vertically (at the 95% level). It proves to have a better accuracy than that of the phase smoothed approach, by about 30% to 50%. In favourable conditions, the accuracy gets close to 4 decimetres horizontally and 6 decimetres vertically (95%), and does not depend on the receiver's dynamics.

At this level of accuracy, other sources of errors should be accounted for. They are solid earth tides, ocean loading, phase wind-up and others. The full correction of satellite antenna phase centre also should be applied. All those corrections/modelling might bring the accuracy close to sub-decimetre level since the errors are at a few decimetres level in total.

Moreover, the GIMs cannot completely eliminate the ionospheric errors. Due to residual ionospheric delays, ionospheric divergence occurs in all the three algorithms. Note that the ionospheric delay was not included in the vector of unknown parameters.

In the stochastic model, the code noise is assumed to be white noise, i.e. no time-correlation between epochs. However, in practice, not all receivers provide white noise pseudoranges as discussed in Bona (2000) (the Trimble 4700 used in the static test was found to have white noise pseudoranges [ibid]). For a receiver without white noise characteristic, i.e. there is time correlation between epochs, current modelling is still sub-optimal.

Multipath is also a significant error source that needs to be considered since it is not included in the model. In certain aspects and depending on the time scale, it could be regarded as both a functional and stochastic error as it contains both a bias and random component.

References

Bona, P. (2000). Precision, cross correlation and time correlation of GPS phase and code observations. GPS Solutions, Vol. 4, No. 2, pp. 3-13.

Bisnath, S.B., T. Beran and R.B. Langley (2002). Precise platform positioning with a single GPS receiver. GPS World, April 2002, pp. 42-49.

Hatch, R. (1982). The Synergism of GPS code and carrier measurements. Proceedings of the 3rd International Geodetic Symposium on Satellite Doppler Positioning, Vol. 2. Las Cruces - New Mexico, 1982, pp. 1213-1231.

Le, A.Q. (2004). Achieving Decimetre Accuracy with Single Frequency Standalone GPS Positioning. Proceedings of the ION GNSS 17th International Technical Meeting of the Satellite Division, 21-24 Sept. 2004, Long Beach, CA, pp. 1881-1892.

Teunissen, P.J.G. (1991). The GPS phase-adjusted pseudorange. Proceedings of the 2nd International Workshop on High Precision Navigation. Stuttgart/Freudenstadt, 1991, pp. 115-125.